Inorganic Chemistry

Synthesis, Structures, and Kinetics of Mixed-Donor Amido–Amino–Siloxo Ligands from Symmetrical Diamidosilyl Ether Ligands via a Retro-Brook Rearrangement

Farzad Haftbaradaran,[†] Angela M. Kuchison,[†] Michael J. Katz,[†] Gabriele Schatte,[‡] and Daniel B. Leznoff*,[†]

Department of Chemistry, Simon Fraser University, Burnaby, British Columbia, Canada V5A 1S6, and Saskatchewan Structural Sciences Center, University of Saskatchewan, Saskatoon, Saskatchewan, Canada S7N 5C9

Deprotonation of the new (R = propyl, 3,5-Me$_2$Ph) and previously prepared (R = 2,4,6-Me$_3$Ph, 2,6-^{i}Pr$_2$Ph, 3,5-(CF$_3$)$_2$Ph) symmetrical diamidosilyl ether ligand precursors {[RNHSiMe$_2$]$_2$O} with 2 equiv of ^{n}BuLi in THF resulted in a new class of mixed-donor amido–amino–siloxo ligands of the form {RNLiSiMe$_2$N(R)SiMe$_2$OLi} (R= propyl (**1c**), 3,5-Me$_2$Ph (**2c**), 2,4,6-Me$_3$Ph (**3c**), 2,6-^{i}Pr$_2$Ph (**4c**), 3,5-(CF$_3$)$_2$Ph (**5c**)) in one-step and high yield via a retro-Brook-type rearrangement mechanism. Ligands **1c**, **3c**, and **4c** have been structurally characterized in the presence and absence of THF/ether donor solvents and exhibited a range of aggregated structures with ring-laddering, ring-stacking, and cubane motifs; higher-nuclearity clusters for base-free systems were observed for **1c** and **4c**. ^{1}H, ^{7}Li, and selected ^{13}C{^{1}H} NMR spectra in THF-d_8 and toluene-d_8 are described; the ^{7}Li data are indicative of intramolecular fluxional behavior as a function of temperature but do not shed light on the nuclearity of the salts in solution. Reaction kinetics were investigated by variable-temperature ^{1}H NMR spectroscopy and showed that the rate of rearrangement reactions increases with decreasing steric hindrance and with increasing electron-donating ability of the R substituents, with $\tau_{1/2}$ values ranging from 5.7×10^1 to 1.5×10^8 s for **2c** and **5c**, respectively.

Introduction

Amido and alkoxo groups are ubiquitous ancillary ligands in inorganic and organometallic chemistry,[1–5] and their metal complexes have a wide variety of applications.[3,6–12] Given this widespread exploitation, there is a noticeable absence of mixed-donor ligands containing both functionalities.[13–16] This could be due to the fact that, in order to modify the substituents of each donor group independently or assemble two or more dissimilar building blocks as would be necessary to synthesize nonsymmetrical mixed-donor ligands, a more challenging, often multistep procedure is usually required.[17] As a particular example, silyl R-group-containing

* To whom correspondence should be addressed. Tel: 1-778-782-4887. Fax: 1-778-782-3765. E-mail: dleznoff@sfu.ca.
† Simon Fraser University.
‡ University of Saskatchewan.

(1) Lappert, M. F.; Power, P. P.; Sanger, A. R.; Srivastava, R. C. *Metal and Metalloid Amides*; Ellis Horwood: Chichester, 1980.
(2) Kempe, R. *Angew. Chem., Int. Ed.* **2000**, *39*, 468.
(3) Chisholm, M. H.; Rothwell, I. P. In *Comprehensive Coordination Chemistry*, 1st ed.; Wilkinson, G., Gillard, R. D., McCleverty, J. A., Eds.; Pergamon Press: Oxford, 1987; Vol. 2, p 161.
(4) Bradley, D. C.; Mehrotra, R. C.; Rothwell, I. P.; Singh, A. *Alkoxo and Aryloxo Derivatives of Metals*; Academic Press: London, 2001.
(5) Bezombes, J. P.; Hitchcock, P. B.; Lappert, M. F.; Merle, P. G. *J. Chem. Soc., Dalton Trans.* **2001**, 816.
(6) Fryzuk, M. D.; Montgomery, C. D. *Coord. Chem. Rev.* **1989**, *95*, 1.
(7) Gary, M.; Tinkl, M.; Snieckus, V. In *Comprehensive Organometallic Chemistry*, 2nd ed.; Abel, E. W., Stone, F. G., Wilkinson, G., Eds.; Pergamon Press: Oxford, 1995; Vol. 11, p 1.
(8) Wright, D. S.; Beswick, M. A. In *Comprehensive Organometallic Chemistry II*; Abel, E. W., Stone, F. G., Wilkinson, G., Eds.; Pergamon: Oxford, 1995; Vol. 1, p 1.
(9) Ruhlandt-Senge, K.; Henderson, K. W.; Andrews, P. C. In *Comprehensive Organometallic Chemistry III*, 1st ed.; Mingos, D. M. P., Crabtree, R. H., Eds.; Elsevier: Oxford, 2007; Vol. 2, p 1.
(10) Lappert, M. F.; Slade, M. J.; Singh, A.; Atwood, J. L.; Rogers, R. D.; Shakir, R. *J. Am. Chem. Soc.* **1983**, *105*, 302.
(11) Stowell, J. C. *Carbanions in Organic Synthesis*; Wiley-Interscience: New York, 1979.
(12) Fieser, M. *Reagents for Organic Synthesis*; Wiley: New York, 1990; Vol. 15 and proceeding volumes.
(13) Rhodes, B.; Chien, J. C. W.; Wood, J. S.; Chandrasekaran, A.; Rausch, M. D. *J. Organomet. Chem.* **2001**, *625*, 95.
(14) Collins, T. J.; Gordon-Wylie, S. W. *J. Am. Chem. Soc.* **1989**, *111*, 4511.
(15) Nonoyama, K.; Mori, W.; Nakajima, K.; Nonoyama, M. *Polyhedron* **1997**, *16*, 3815.
(16) Holland, R.; Jeffery, J. C.; Russell, C. A. *J. Chem. Soc., Dalton Trans.* **1999**, 3331.
(17) Fryzuk, M. D.; Giesbrecht, G. R.; Johnson, S. A.; Kickham, J. E.; Love, J. B. *Polyhedron* **1998**, *17*, 947.

silylamido-,[2,18] siloxo-,[19,20] and silsesquioxo-type[21−23] ligands are extremely widespread, yet there are very few ligands that incorporate both silylamido and siloxo donors,[13−15] perhaps due to the potential difficulties in isolating putative amino/ Si−OH intermediates.

In this light, we recently reported the facile, high-yield preparation of two nonsymmetrical mixed-donor amido− amino−siloxo ligands of the form {RNLiSiMe$_2$N(R)SiMe$_2$- OLi}, termed [^{R}NN′O]$^{2−}$, containing the bulky, electron-rich R-groups 2,4,6-Me$_3$Ph and 2,6-^{i}Pr$_2$Ph.[24] The synthesis utilizes a 1,3-silyl retro-Brook rearrangement of the corresponding symmetrical diamidosilyl ether ligands {[RNSiMe$_2$]$_2$O}$^{2−}$, termed [^{R}NON]$^{2−}$. Such Brook-type silyl migrations have been studied extensively in the past;[25−29] however, to the best of our knowledge, the value of the anionic products of such reactions as new ligands has not been previously considered.[30] Since diamidosilyl ether [^{R}NON]$^{2−}$ ligands can be easily modified via the nitrogen substituent to achieve a range of steric and electronic profiles,[31−38] we perceived these diamido chelates to be potential starting materials for many other amido−siloxo-type ligands that would otherwise be synthetically challenging to access. Thus, the main goal of this contribution was to probe the generality of this retro-Brook rearrangement reaction by targeting the synthesis of new Li$_2$[^{R}NN′O] ligands with R-groups spanning a range of steric and electronic character, as shown in Scheme 1.

In addition, the synthesis of this rare class of mixed-donor amido−siloxo ligands as their dilithium salts provided the opportunity to examine their structural chemistry, both in the presence and absence of a coordinating solvent.[1,39−41] There has been great interest in the structural characterization

Scheme 1
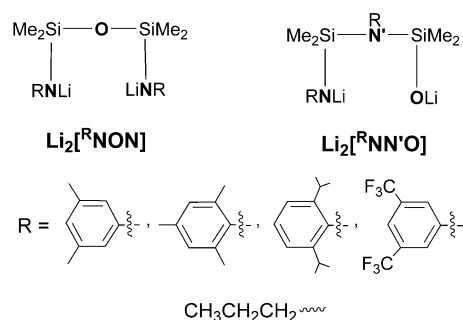
of lithium amides and alkoxides.[42−44] Many fascinating structures and levels of aggregation have been reported, the degree of which often translates to the reactivity of these compounds;[5,10,45] this clustering in solution and the solid phase is due to the relatively high polarity of the Li−X (X = N, O) bond.[46−49] However, although the structural chemistry and aggregation of simple amides, siloxides/ alkoxides, and symmetrical dianionic ligands have been well-explored, the general lack of mixed amido−siloxo ligands has precluded any analogous investigation of their structural chemistry. With a systematic series of such Li$_2$[^{R}NN′O] ligands in hand, the factors influencing the structural chemistry for such mixed-donor ligands are also described herein.

Experimental Section

General Procedures, Materials, and Instrumentation. All reactions were carried out under an inert atmosphere of dry nitrogen gas using standard Schlenk and vacuum line or glovebox (mBraun Labmaster 130) techniques. Hexanes and toluene (Fisher) were passed through an mBraun solvent purification system connected to a glovebox. The tetrahydrofuran, THF (Caledon), was distilled from a potassium/benzophenone mixture under a nitrogen atmosphere. The diethyl ether, Et$_2$O (Caledon), was distilled from a sodium/benzophenone mixture under a nitrogen atmosphere. All glassware including the NMR test tubes were dried overnight prior to use. Benzene-d_6 (Aldrich), toluene-d_8 (Aldrich), and THF-d_8 (Cambridge Isotope Laboratories) were dried over activated 4 Å molecular sieves (Acros)/sodium and stored under a nitrogen atmosphere. Anhydrous pentane (Aldrich) was dried with KH (Aldrich), filtered over dried neutral alumina (Fisher) and stored under a nitrogen atmosphere. Amines were passed through a column of dried neutral alumina (Fisher) prior to use. All other reagents

(18) Gibson, V. C.; Spitzmesser, S. K. *Chem. Rev.* **2003**, *103*, 283.
(19) King, L. *Coord. Chem. Rev.* **1999**, *189*, 19.
(20) Marciniec, B.; Maciejewski, M. *Coord. Chem. Rev.* **2001**, *223*, 301.
(21) Feher, F. J.; Budzichowski, T. A. *Polyhedron* **1995**, *14*, 3239.
(22) Abbenhuis, H. C. L. *Chem. Eur. J.* **2000**, *6*, 25.
(23) Hanssen, R. W. J. M.; van Santen, R. A.; Abbenhuis, H. C. L. *Eur. J. Inorg. Chem.* **2004**, 675.
(24) Haftbaradaran, F.; Mund, G.; Batchelor, R. J.; Britten, J. F.; Leznoff, D. B. *Dalton Trans.* **2005**, 2343.
(25) Brook, A. G.; Bassindale, A. R. In *Rearrangements in Ground and Excited States*; de Mayo, P., Ed.; Academic Press: New York, 1980; Vol. 42-2, p 149.
(26) Brook, M. A. *Silicon in Organic, Organometallic, and Polymer Chemistry*; Wiley-Interscience: New York, 2000.
(27) Brook, A. G. *Acc. Chem. Res.* **1974**, *7*, 77.
(28) West, R.; Lowe, R.; Stewart, H. F.; Wright, A. *J. Am. Chem. Soc.* **1971**, *93*, 282.
(29) Bush, R. P.; Lloyd, N. C.; Pearce, C. A. *Chem. Commun. (London)* **1968**, *19*, 1191.
(30) Katti, K. V.; Pinkerton, A. A.; Cavell, R. G. *Inorg. Chem.* **1991**, *30*, 2631.
(31) Leznoff, D. B.; Mund, G.; Jantunen, K. C.; Bhatia, P. H.; Gabert, A. J.; Batchelor, R. J. *J. Nuc. Sci. Technol.* **2002**, *Suppl. 3*, 406.
(32) Mund, G.; Vidovic, D.; Batchelor, R. J.; Britten, J. F.; Sharma, R. D.; Jones, C. H. W.; Leznoff, D. B. *Chem. Eur. J.* **2003**, *9*, 4757.
(33) Mund, G.; Batchelor, R. J.; Sharma, R. D.; Jones, C. H. W.; Leznoff, D. B. *Dalton Trans.* **2002**, 136.
(34) Jantunen, K. C.; Batchelor, R. J.; Leznoff, D. B. *Organometallics* **2004**, *23*, 286.
(35) Male, N. A. H.; Thornton-Pett, M.; Bochmann, M. *J. Chem. Soc. Dalton. Trans* **1997**, 2487.
(36) Elias, A. J.; Schmidt, H. G.; Noltemeyer, M.; Roesky, H. W. *Eur. J. Solid State Inorg. Chem.* **1992**, *29*, 23.
(37) Das, A. K.; Moatazedi, Z.; Mund, G.; Batchelor, R. J.; Bennett, A. J.; Leznoff, D. B. *Inorg. Chem.* **2007**, *46*, 366.
(38) Elias, A. J.; Roesky, H. W.; Robinson, W. T.; Sheldrick, G. M. *J. Chem. Soc., Dalton Trans.* **1993**, 495.
(39) Wakefield, B. J. *The Chemistry of Organolithium Compounds*; Pergamon Press: Oxford, 1974.
(40) Wardell, J. L. In *Comprehensive Organometallic Chemistry*, 1st ed.; Abel, E. W., Wilkinson, G., Stone, F. G. A., Eds.; Pergamon Press: Oxford; New York, 1982; Vol. 1, p 43.
(41) Sapse, A.-M.; Schleyer, P. v. R. *Lithium Chemistry: A Theoretical and Experimental Overview*; Wiley-Interscience: New York, 1995.
(42) Setzer, W.; Schleyer, P. v. R. *Adv. Organomet. Chem.* **1985**, *24*, 353.
(43) Mulvey, R. E. *Chem. Soc. Rev.* **1991**, *20*, 167.
(44) Gregory, K.; Schleyer, P. v. R.; Snaith, R. *Adv. Inorg. Chem.* **1991**, *37*, 47.
(45) Olsher, U.; Izatt, R. M.; Bradshaw, J. S.; Dalley, N. K. *Chem. Rev.* **1991**, *91*, 137.
(46) Collum, D. B. *Acc. Chem. Res.* **1993**, *26*, 227.
(47) Mulvey, R. E. *Chem. Soc. Rev.* **1998**, *27*, 339.
(48) Clegg, W.; Liddle, S. T.; Mulvey, R. E.; Robertson, A. *J. Chem. Soc., Chem. Commun.* **1999**, 511.
(49) Clegg, W.; Henderson, K. W.; Horsburgh, L.; Mackenzie, F. M.; Mulvey, R. E. *Chem. Eur. J.* **1998**, *4*, 53.

were used as received. The ligands [RNHSiMe$_2$]$_2$O (R = 2,4,6-Me$_3$Ph (H$_2$[^{Me_3Ph}NON], **3a**);[31] R = 2,6-^{i}Pr$_2$Ph (H$_2$[^{iPr_2Ph}NON], **4a**);[31,33] R = 3,5-(CF$_3$)$_2$Ph (H$_2$[^{CF_3Ph}NON], **5a**);[31,33] R = ^{t}Bu (H$_2$-[^{tBu}NON])[35,36] and Li$_2$\{[^{t}BuNSiMe$_2$]$_2$O\} (Li$_2$[^{tBu}NON])[50,51] were prepared from published procedures. Monolithiated 3,5-dimethylaniline (3,5-Me$_2$PhNHLi) was prepared by stoichiometric addition of ^{n}BuLi to an ether solution of 3,5-dimethylaniline at −78 °C followed by stirring for 5 h, solvent removal in vacuo, and a pentane wash.

NMR spectra were recorded at 298 K, unless otherwise stated, in benzene-d_6, toluene-d_8, or THF-d_8 employing a 500 MHz Varian Unity spectrometer (^{1}H, ^{13}C\{^{1}H\}), a 600 MHz Bruker AMX spectrometer (^{13}C\{^{1}H\}, ^{1}H VT), or a 600 MHz Bruker Avance II spectrometer (^{7}Li, VT). The temperature at the position of the sample was calibrated using a standard methanol sample, with an error of ±1 K. All ^{1}H chemical shifts are reported in ppm and referenced to benzene-d_6, δ 7.16 (^{1}H), toluene-d_8, δ 2.09 (^{1}H) and 137.86 (^{13}C\{^{1}H\}), and THF-d_8, δ 3.58 (^{1}H) and 67.57 (^{13}C\{^{1}H\}). All ^{7}Li chemical shifts are reported in ppm relative to an external standard solution of LiCl in D$_2$O (δ 0.0, ^{7}Li). NMR data were processed with MESTREC NMR data processing software (MESTRECLAB research). Elemental analyses (C, H, and N) were performed by Mr. Miki Yang (SFU) employing a Carlo Erba EA 1110 CHN elemental analyzer. Mass spectra were measured using a HP-5985 GC-MS CI instrument operating at 70 eV by Mr. Phil Ferreira (SFU).

H$_2$[^{Pr}NON] (1a). 1,3-Dichloro-1,1,3,3-tetramethyldisiloxane (3.0 mL, 15.3 mmol) was added dropwise to an excess of neat anhydrous propylamine (9.07 g, 153 mmol) at 0 °C while stirring. The resulting white mixture was stirred overnight, and then the excess propylamine was removed in vacuo. The product was extracted with hexanes and filtered through Celite. The removal of hexanes in vacuo resulted in a clear colorless oil of **1a**. Yield: 3.32 g (87%). Anal. Calcd for C$_{10}$H$_{28}$N$_2$OSi$_2$: C, 48.33; H, 11.36; N, 11.27. Found: C, 48.20; H, 11.26; N, 11.16. ^{1}H NMR (benzene-d_6): δ 0.18 (s, 12H, Si(CH$_3$)$_2$), 0.67 (br s, 2H, N−H), 0.84 (t, 6H, $^3J_{HH}$ = 7.3 Hz, CH$_2$CH$_2$CH$_3$), 1.35 (m, 4H, CH$_2$CH$_2$CH$_3$), 2.72 (m, 4H, CH$_2$CH$_2$CH$_3$). ^{13}C\{^{1}H\} NMR (toluene-d_8): δ 0.27 (Si(CH$_3$)$_2$), 11.92 (CH$_2$CH$_2$CH$_3$), 28.53 (CH$_2$CH$_2$CH$_3$), 44.03 (CH$_2$CH$_2$CH$_3$). ^{13}C\{^{1}H\} NMR (THF-d_8): δ −0.80 (Si(CH$_3$)$_2$), 11.06 (CH$_2$CH$_2$CH$_3$), 27.96 (CH$_2$CH$_2$CH$_3$), 43.52 (CH$_2$CH$_2$CH$_3$). MS (CI): m/z 249 (M$^+$), 234 (M$^+$ − Me), 190 (M$^+$ − Me − Pr).

H$_2$[^{Me_2Ph}NON] (2a). A green solution of 3,5-Me$_2$PhNHLi (5.227 g, 41 mmol) in 150 mL of Et$_2$O was cooled to −30 °C, and 1,3-dichloro-1,1,3,3-tetramethyldisiloxane (4.0 mL, 20 mmol) in 15 mL of Et$_2$O was added dropwise. Gradually, the reaction became cloudy orange. The reaction was warmed to room temperature and stirred overnight. The solvent was removed in vacuo and the residue was extracted with hexanes and filtered through Celite. The hexanes were removed in vacuo to obtain a dark orange oil of **2a**. Yield: 6.907 g (90%). Anal. Calcd for C$_{20}$H$_{32}$N$_2$OSi$_2$: C, 64.46; H, 8.66; N, 7.52. Found: C, 64.68; H, 8.54; N, 7.45. ^{1}H NMR (benzene-d_6): δ 0.25 (s, 12H, Si(CH$_3$)$_2$), 2.17 (s, 12H, m-CH$_3$), 3.39 (br s, 2H, N-H), 6.38 (s, 4H, o-H), 6.43 (s, 2H, p-H). MS (CI): m/z 372 (M$^+$ − H).

Li$_2$[^{Pr}NON] (1b). A clear, colorless oil of **1a** (5.000 g, 20.2 mmol) was dissolved in 30 mL of Et$_2$O, and 2 equiv of 1.6 M ^{n}BuLi in hexanes (25.15 mL, 40.3 mmol) was added dropwise at −78 °C, yielding a white mixture. After being stirred for 2 h at

room temperature, the solvent was removed in vacuo and the resulting white residue was brought into the glovebox. Hexanes (20 mL) were added, and the resulting suspension was filtered on a frit filter and dried in vacuo to obtain a white powder of **1b**. Yield: 5.074 g (93%). Anal. Calcd for C$_{10}$H$_{26}$N$_2$Li$_2$OSi$_2$: C, 46.13; H, 10.06; N, 10.76. Found: C, 46.41; H, 10.09; N, 10.48. ^{1}H NMR (THF-d_8): δ −0.15 (s, 12H, Si(CH$_3$)$_2$), 0.78 (t, 6H, $^3J_{HH}$ = 7.2 Hz, CH$_2$CH$_2$CH$_3$), 1.29 (m, 4H, CH$_2$CH$_2$CH$_3$), 2.87 (m, 4H, CH$_2$CH$_2$CH$_3$). ^{13}C\{^{1}H\} NMR (THF-d_8): δ 2.09 (Si(CH$_3$)$_2$), 11.49 (CH$_2$CH$_2$CH$_3$), 32.74 (CH$_2$CH$_2$CH$_3$), 50.63 (CH$_2$CH$_2$CH$_3$).

Li$_2$[^{Me_2Ph}NON] (2b). A dark orange oil of **2a** (3.000 g, 8.05 mmol) was dissolved in 60 mL of Et$_2$O, and 2 equiv of 1.6 M ^{n}BuLi in hexanes (10.1 mL, 16.1 mmol) was added dropwise at −78 °C, yielding a light yellow mixture. After being stirred for 30 min at room temperature, the solvent was removed in vacuo and the resulting residue was brought into the glovebox. Hexanes (30 mL) were added, and the resulting suspension was filtered on a frit filter and dried in vacuo to obtain a white powder of **2b**. Yield: 2.793 g (90%). Anal. Calcd for C$_{20}$H$_{30}$N$_2$Li$_2$OSi$_2$: C, 62.47; H, 7.86; N, 7.28. Found: C, 62.16; H, 8.05; N, 6.96. ^{1}H NMR (THF-d_8): δ 0.12 (s, 12H, Si(CH$_3$)$_2$), 2.08 (s, 12H, m-CH$_3$), 5.94 (s, 2H, p-H), 6.18 (s, 4H, o-H).

Li$_2$[^{Me_3Ph}NON] (3b). A colorless solid of **3a** (4.230 g, 10.6 mmol) was dissolved in 50 mL of Et$_2$O, and 2 equiv of 1.6 M ^{n}BuLi in hexanes (13.2 mL, 21.1mmol) was added dropwise at −78 °C, yielding a white mixture. The reaction was warmed to room temperature and stirred overnight. The solvent was removed in vacuo, and the resulting residue was brought into the glovebox. Hexanes (30 mL) were added, and the resulting suspension was filtered on a frit filter and dried in vacuo to obtain a white powder of **3b**. Yield: 4.005 g (92%). Anal. Calcd for C$_{22}$H$_{34}$N$_2$Li$_2$OSi$_2$: C, 64.05; H, 8.31; N, 6.79. Found: C, 63.79; H, 8.24; N, 6.69. ^{1}H NMR (THF-d_8): δ −0.12 (s, 12H, Si(CH$_3$)$_2$), 2.04 (s, 6H, p-CH$_3$), 2.17 (s, 12H, o-CH$_3$), 6.51 (s, 4H, aromatic H).

Li$_2$[^{iPr_2Ph}NON] (4b). A clear, colorless oil of **4a** (5.270 g, 10.9 mmol) was diluted in 50 mL of ether, cooled to −78 °C, and 2 equiv of 1.6 M ^{n}BuLi in hexanes (13.6 mL, 21.7 mmol) was added dropwise. Immediately, a white solid formed. The reaction was warmed to room temperature and stirred for 18 h. The solvent was removed in vacuo, and the remaining residue was brought into the glovebox. Hexanes (30 mL) were added, and the resulting suspension was filtered on a frit filter and dried in vacuo to obtain a white powder of **4b**. Yield: 4.180 g (77%). Anal. Calcd for C$_{28}$H$_{46}$N$_2$Li$_2$OSi$_2$: C, 67.70; H, 9.33; N, 5.64. Found: C, 67.89; H, 9.22; N, 5.53. ^{1}H NMR (THF-d_8): δ −0.07 (s, 12H, Si(CH$_3$)$_2$), 1.05 (d, 24H, $^3J_{HH}$ = 6.8 Hz, CH(CH$_3$)$_2$), 4.18 (m, 4H, CH(CH$_3$)$_2$), 6.18 (t, 2H, $^3J_{HH}$ = 7.0 Hz, p-H), 6.65 (d, 4H, $^3J_{HH}$ = 6.9 Hz, m-H).

Li$_2$[^{CF_3Ph}NON] (5b). A dark brown oil of **5a** (5.030 g, 8.6 mmol) was diluted in 50 mL of hexanes and cooled to −30 °C, and 2 equiv of 1.6 M ^{n}BuLi in hexanes (10.6 mL, 17 mmol) was added dropwise, yielding a cloudy brown mixture. The reaction was warmed to room temperature and stirred overnight. The solvent was removed in vacuo, and the remaining residue was brought into the glovebox. Hexanes (30 mL) were added, and the resulting suspension was filtered on a frit filter and dried in vacuo to obtain a light brown powder of **5b**. Yield: 3.850 g (76%). Anal. Calcd. for C$_{20}$H$_{18}$N$_2$F$_{12}$Li$_2$OSi$_2$: C, 40.01; H, 3.02; N, 4.67. Found: C, 40.39; H, 3.40; N, 4.67. ^{1}H NMR (THF-d_8): δ 0.07 (s, 12H, Si-(CH$_3$)$_2$), 6.23 (s, 2H, p-H), 6.73 (s, 4H, o-H).

Li$_2$[^{Pr}NN'O] (1c). A white solid of **1b** (1.500 g, 5.76 mmol) was dissolved in 20 mL of THF and stirred at 70 °C for 72 h. The solvent was then removed in vacuo, and the resulting powder washed with a minimum amount of hexanes and dried to obtain a

(50) Veith, M.; Wieczorek, S.; Fries, K.; Huch, V. *Z. Anorg. Allg. Chem.* **2000**, *626*, 1237.

(51) Ikeda, H.; Monoi, T.; Nakayama, Y.; Yasuda, H. *J. Organomet. Chem.* **2002**, *642*, 156.

white powder of **1c**. Yield: 1.381 g (92%). Anal. Calcd for $C_{10}H_{26}N_2Li_2OSi_2$: C, 46.13; H, 10.06; N, 10.76. Found: C, 46.50; H, 9.94; N, 10.40. ^{1}H NMR (toluene-d_8): δ 0.27 (s, 6H, Si(CH_3)$_2$), 0.38 (s, 6H, Si(CH_3)$_2$), 0.77 (t, 3H, $^3J_{HH}$ = 7.4 Hz, CH$_2$CH$_2$CH_3), 0.97 (t, 3H, $^3J_{HH}$ = 7.3 Hz, CH$_2$CH$_2$CH_3), 1.46 (m, 4H, CH$_2$CH_2-CH$_3$), 2.76 (m, 2H, CH_2CH$_2$CH$_3$), 3.12 (m, 2H, CH_2CH$_2$CH$_3$). ^{1}H NMR (THF-d_8): δ −0.10 (s, 6H, Si(CH_3)$_2$), −0.06 (s, 6H, Si(CH_3)$_2$), 0.73 (t, 3H, $^3J_{HH}$ = 7.4 Hz, CH$_2$CH$_2$CH_3), 0.80 (t, 3H, $^3J_{HH}$ = 7.3 Hz, CH$_2$CH$_2$CH_3), 1.35 (m, 4H, CH$_2$CH_2CH$_3$), 2.59 (m, 2H, CH_2CH$_2$CH$_3$), 2.85 (m, 2H, CH_2CH$_2$CH$_3$). ^{13}C{^{1}H} NMR (toluene-d_8): δ 2.64, 2.77, 3.02, 4.58 (Si(CH_3)$_2$), 11.42, 11.53 (CH$_2$CH$_2$CH$_3$), 27.96, 31.63 (CH$_2$CH$_2$CH$_3$), 47.02, 48.71 (CH$_2$CH$_2$CH$_3$). ^{13}C{^{1}H} NMR (THF-d_8): δ 1.30, 3.19 (Si(CH_3)$_2$), 11.02, 11.46 (CH$_2$CH$_2$CH$_3$), 28.13, 31.74 (CH$_2$CH$_2$CH$_3$), 47.08, 51.50 (CH$_2$CH$_2$CH$_3$). ^{7}Li NMR (toluene-d_8): δ 0.74, 1.41, 1.53 (2:2:1 integration). ^{7}Li NMR (THF-d_8): δ −1.28, −1.18, −1.03 (1:1:7 integration); ^{7}Li NMR (THF-d_8, 173 K): δ −1.15, −1.05 (1:1 integration). Single crystals of **1c** were obtained from the slow, partial evaporation of a saturated toluene/pentane solution in the glovebox and of **1c·2THF** from a saturated THF/toluene solution. The product **1c** can also be obtained by a one-pot reaction of diamine **1a** and 2 equiv of ^{n}BuLi in THF at −78 °C followed by stirring at 70 °C for 72 h.

Li$_2$[^{Me_2Ph}NN′O] (2c). A white solid of **2b** (0.300 g, 0.78 mmol) was dissolved in 60 mL of THF and stirred at room temperature for 15 min. The THF was then removed in vacuo and the resulting powder was washed with a minimum amount of pentane and dried to obtain a white powder of **2c**. Yield: 0.294 g (98%). Anal. Calcd for $C_{20}H_{30}N_2Li_2OSi_2$: C, 62.47; H, 7.86; N, 7.28. Found: C, 62.34; H, 8.17; N, 6.98. ^{1}H NMR (THF-d_8): δ 0.02 (s, 6H, Si(CH_3)$_2$), 0.40 (s, 6H, Si(CH_3)$_2$), 2.09 (s, 6H, m-CH_3), 2.23 (s, 6H, m-CH_3), 5.94 (s, 1H, p-H), 6.36 (s, 2H, o-H), 6.63 (s, 1H, p-H), 6.69 (s, 2H, o-H). The product **2c** can also be obtained by a one-pot reaction of diamine **2a** and 2 equiv of ^{n}BuLi in THF at −78 °C followed by stirring at room temperature for 15 min.

Li$_2$[^{Me_3Ph}NN′O] (3c). A white solid of **3b** (0.950 g, 2.30 mmol) was dissolved in 15 mL of THF and stirred at room temperature for 2 h. The THF was removed in vacuo and the resulting yellow residue was washed with a minimum amount of hexanes and dried to obtain a white powder of **3c**. Yield: 0.891 g (94%). Anal. Calcd for $C_{22}H_{34}N_2Li_2OSi_2$: C, 64.05; H, 8.31; N, 6.79. Found: C, 64.27; H, 8.59; N, 6.71. ^{1}H NMR (toluene-d_8): δ 0.03 (s, 6H, Si(CH_3)$_2$), 0.15 (s, 6H, Si(CH_3)$_2$), 2.12 (s, 3H, p-CH_3), 2.14 (s, 3H, p-CH_3), 2.18 (s, 6H, o-CH_3), 2.37 (s, 6H, o-CH_3), 6.77 (s, 2H, aromatic H), 6.79 (s, 2H, aromatic H). ^{1}H NMR (THF-d_8): δ −0.33 (s, 6H, Si(CH_3)$_2$), −0.12 (s, 6H, Si(CH_3)$_2$), 2.05 (s, 3H, p-CH_3), 2.15 (s, 3H, p-CH_3), 2.20 (s, 6H, o-CH_3), 2.41 (s, 6H, o-CH_3), 6.55 (s, 2H, aromatic H), 6.67 (s, 2H, aromatic H). ^{7}Li NMR (toluene-d_8): δ 1.51. ^{7}Li NMR (THF-d_8): δ −1.35. ^{7}Li NMR (THF-d_8, 183 K): δ −2.06, −0.68 (1:1 integration). Single crystals of **3c** were obtained from the slow, partial evaporation of a concentrated toluene/hexanes solution in the glovebox, while crystals of **3c·THF** were obtained from a THF/toluene solution. The product **3c** can also be obtained by a one-pot reaction of diamine **3a** and 2 equiv of ^{n}BuLi in THF at −78 °C followed by stirring at room temperature for 2 h.

Li$_2$[^{iPr_2Ph}NN′O] (4c). A white solid of **4b** (1.470 g, 2.96 mmol) was dissolved in 50 mL of THF and stirred at room temperature for 48 h. The solvent was removed in vacuo, and the resulting white powder was washed with a minimum amount of cold hexanes and dried to obtain a white powder of **4c**. Yield: 1.152 g (78%). Anal. Calcd for $C_{28}H_{46}N_2Li_2OSi_2$: C, 67.70; H, 9.33; N, 5.64. Found: C, 67.80; H, 9.45; N, 5.39. ^{1}H NMR (toluene-d_8): δ −0.06 (s, 6H, Si(CH_3)$_2$), 0.10 (s, 6H, Si(CH_3)$_2$), 1.21 (d, 12H, $^3J_{HH}$ = 6.8 Hz, CH(CH_3)$_2$), 1.35 (d, 12H, $^3J_{HH}$ = 6.7 Hz, CH(CH_3)$_2$), 3.77 (m, 2H, CH(CH$_3$)$_2$), 4.00 (m, 2H, CH(CH$_3$)$_2$), 7.01 (d, 2H, $^3J_{HH}$ = 6.7 Hz, m-H), 7.05 (t, 1H, $^3J_{HH}$ = 6.7 Hz, p-H), 7.08 (d, 2H, $^3J_{HH}$ = 6.7 Hz, m-H), 7.13 (t, 1H, $^3J_{HH}$ = 6.7 Hz, p-H). ^{1}H NMR (THF-d_8): δ −0.25 (s, 6H, Si(CH_3)$_2$), −0.07 (s, 6H, Si(CH$_3$)$_2$), 1.07 (d, 12H, $^3J_{HH}$ = 7.6 Hz CH(CH_3)$_2$), 1.24 (d, 12H, $^3J_{HH}$ = 7.6 Hz CH(CH_3)$_2$), 4.14 (m, 2H, CH(CH$_3$)$_2$), 4.26 (m, 2H, CH(CH$_3$)$_2$), 6.18 (t, 1H, $^3J_{HH}$ = 7.8 Hz, p-H), 6.32 (t, 1H, $^3J_{HH}$ = 7.8 Hz p-H), 6.74 (d, 2H, $^3J_{HH}$ = 7.4 Hz, m-H), 6.94 (d, 2H, $^3J_{HH}$ = 7.6 Hz m-H). ^{7}Li NMR (toluene-d_8): δ - 0.41, −0.31 (1:1 integration). ^{7}Li NMR (THF-d_8): δ −1.83, −0.81 (1:1 integration); ^{7}Li NMR (THF-d_8, 323 K): δ −0.86. Single crystals of **4c** were obtained from the slow, partial evaporation of a saturated toluene/hexanes solution in the glovebox, while crystals of **4c·3Et$_2$O** were obtained from an Et$_2$O solution. The product **4c** can also be obtained by a one-pot reaction of diamine **4a** and 2 equiv of ^{n}BuLi in THF at −78 °C followed by stirring at room temperature for 48 h.

Li$_2$[^{CF_3Ph}NN′O] (5c). A light brown powder of **5b** (5.070 g, 8.44 mmol) was dissolved in 50 mL of THF and stirred for 10 days at 70 °C. The solvent was removed in vacuo and the resulting light brown powder was washed with a minimum amount of cold hexanes and dried to obtain a light brown powder of **5c**. Yield: 3.853 g (76%). Anal. Calcd for $C_{20}H_{18}N_2F_{12}Li_2OSi_2$: C, 40.01; H, 3.02; N, 4.67. Found: C, 40.28; H, 2.87; N, 4.93. ^{1}H NMR (THF-d_8): δ 0.07 (s, 6H, Si(CH_3)$_2$), δ 0.09 (s, 6H, Si(CH_3)$_2$), 6.23 (s, 1H, p-H), 6.35 (s, 1H, p-H), 6.83 (s, 2H, o-H), 6.73 (s, 2H, o-H). The product **5c** can also be obtained by a one-pot reaction of diamine **5a** and 2 equiv of ^{n}BuLi in THF at −78 °C followed by stirring at 70 °C for 10 days.

Kinetic Measurements. The rearrangement reactions were carried out in an NMR tube equipped with a Teflon J. Young valve. The N-lithio derivative of the diamidosilyl ether ligands, THF-d_8, and NMR tubes were cooled down to −30 °C to inhibit the start of the rearrangement reaction prior to the first NMR run (except for **1b** and **5b**, which exhibit relatively much slower reaction rates). The NMR samples were prepared by adding 1 mL of THF-d_8 to 20 mg of the N-lithio derivative of the ligand and transferring an adequate amount of solution into the NMR sample tube. Then, the NMR tube was sealed and the first spectra were obtained as soon as possible. More spectra were obtained during the course of the reaction until the reaction was nearly completed. For **1c** and **5c**, the samples were heated in an external temperature-controlled oil bath during the course of the reactions and the NMR spectrum (at room temperature) periodically sampled.

X-ray crystallography. Crystallographic data for all structures are collected in Table 8. The crystals were mounted onto the nylon fiber of a mounted CryoLoop and attached to a metallic pin using epoxy adhesive. Crystal descriptions for each compound are as follows. **3a** is a colorless block having dimensions 0.25 × 0.20 × 0.20 mm^3; **1c** is a colorless prism having dimensions 0.32 × 0.30 × 0.22 mm^3; **1c·2THF** is a colorless plate having dimensions 0.30 × 0.25 × 0.20 mm^3; **3c** is a colorless plate having dimensions 0.15 × 0.15 × 0.10 mm^3; **3c·THF** is a colorless block having dimensions 0.20 × 0.20 × 0.18 mm^3; **4c** is a colorless plate having dimensions 0.20 × 0.15 × 0.10 mm^3; **4c·3Et$_2$O** is a colorless block having dimensions 0.20 × 0.20 × 0.18 mm^3. The crystal was then transferred to the cold stream of the X-ray diffractometer.

Measurements for **3a**, **1c·2THF**, **3c**, **3c·THF**, **4c**, and **4c·3Et$_2$O** were made on a Nonius KappaCCD 4-Circle Kappa FR540C diffractometer using monochromated Mo Kα radiation (λ = 0.71073 Å) at −100 °C. Compound **1c** was collected on a Bruker SMART APEX II diffractometer using monochromated Mo Kα radiation (λ = 0.71073 A) at −150 °C. Data reduction and absorption

Table 1. Selected Interatomic Distances (Å) and Bond Angles (deg) for **3a**

Si(1)−C(1)	1.845(3)	Si(2)−C(4)	1.848(2)
Si(1)−C(2)	1.852(3)	Si(2)−N(2)	1.711(2)
Si(1)−N(1)	1.711(2)	Si(2)−O(1)	1.6316(15)
Si(1)−O(1)	1.6276(16)	N(1)−C(10)	1.427(3)
Si(2)−C(3)	1.851(2)	N(2)−C(20)	1.425(3)
O(1)−Si(1)−N(1)	112.87(9)	Si(1)−N(1)−C(10)	127.61(15)
C(1)−Si(1)−C(2)	113.85(16)	Si(2)−N(2)−C(20)	128.72(15)
O(1)−Si(2)−N(2)	112.99(9)	Si(1)−O(1)−Si(2)	144.37(10)

Table 2. Selected Interatomic Distances (Å) and Bond Angles (deg) for **1c**

Si(1D)−N(1D)	1.7569(13)	N(2D)−Li(6)	2.101(3)
Si(1D)−O(1D)	1.6168(10)	N(2D)−C(8D)	1.4820(18)
Si(2D)−N(1D)	1.7690(12)	N(2D)−Li(7)	2.084(3)
Si(2D)−N(2D)	1.7022(13)	O(1B)−Li(8)	2.050(3)
N(2B)−Li(8)	2.043(3)	O(1B)−Li(6)	2.006(3)
N(2B)−Li(7)	2.050(3)	O(1A)−Li(6)	1.975(3)
N(1D)−Li(7)	2.224(3)	O(1D)−Li(5)	2.000(3)
N(2D)−Li(8)	2.019(3)		
N(1D)−Si(2D)−N(2D)	105.25(6)	Li(5)−O(1D)−Li(6)	78.69(10)
Li(3)−O(1D)−Li(7)	159.42(11)	Si(1D)−N(1D)−Si(2D)	124.27(7)
Li(8)−N(2D)−Li(7)	65.76(10)	N(2D)−Li(7)−N(2B)	112.53(12)
N(2D)−Li(8)−N(2B)	115.63(13)	Li(7)−N(2B)−Li(8)	65.96(11)
N(2B)−Li(8)−O(1B)	95.62(11)	O(1B)−Li(5)−N(2B)	93.39(11)
O(1B)−Li(6)−O(1D)	101.09(11)		

Table 3. Selected Interatomic Distances (Å) and Bond Angles (deg) for **1c·2THF**

N(21)−Si(1)	1.7511(15)	O(1)−Li(1)[a]	1.869(3)
N(21)−Si(2)	1.7345(15)	O(1)−Li(2)	1.942(3)
N(31)−C(31)	1.465(2)	O(1)−Li(2)*	1.996(3)
N(31)−Li(1)	1.991(3)	O(1)−Si(2)	1.6106(12)
N(31)−Li(2)	2.067(3)	O(2)−Li(1)	1.956(3)
N(31)−Si(1)	1.6847(15)	O(3)−Li(2)	2.020(3)
N(21)−Si(1)−N(31)	113.25(7)	Si(1)−N(31)−Li(1)	104.71(12)
O(1)−Si(2)−N(21)	113.45(7)	Si(1)−N(31)−C(31)	119.30(12)
Si(2)−O(1)−Li(1)[a]	125.96(12)	N(31)−Li(1)−O(1)[a]	106.28(16)
Si(2)−O(1)−Li(2)	111.08(11)	N(31)−Li(1)−O(2)	131.48(18)
Si(2)−O(1)−Li(2)[a]	137.43(11)	N(31)−Li(2)−O(1)	108.64(15)
Li(1)*−O(1)−Li(2)	115.75(15)	N(31)−Li(2)−O(3)	113.67(15)
Li(1)*−O(1)−Li(2)[a]	78.96(14)		

[a] Symmetry transformations used to generate equivalent atoms: $-x + 1, -y, -z + 2$.

Table 4. Selected Interatomic Distances (Å) and Bond Angles (deg) for **3c**

Si(1)−O(1)	1.601(2)	N(31)−Si(2)	1.777(3)
Si(1)−N(31)	1.774(3)	N(41)−Li(4)	2.099(6)
Si(3)−O(2)	1.600(2)	N(51)−Li(3)	2.283(6)
Si(4)−N(41)	1.722(3)	O(1)−Li(1)	1.989(6)
Si(4)−N(51)	1.776(3)	O(1)−Li(2)	1.897(7)
N(21)−C(20)	1.437(4)	O(1)−Li(3)	1.843(6)
N(21)−Li(1)	2.117(6)	C(20)−Li(4)	2.430(6)
N(21)−Li(2)	2.082(7)	C(20)−C(21)	1.430(5)
N(21)−Li(4)	2.229(6)	C(21)−C(22)	1.384(5)
N(31)−Li(1)	2.257(6)	C(22)−C(23)	1.381(6)
O(1)−Si(1)−N(31)	104.31(13)	C(20)−N(21)−Li(4)	79.9(2)
N(21)−Si(2)−N(31)	103.92(13)	Si(1)−N(31)−Si(2)	123.17(15)
Si(1)−O(1)−Li(1)	94.35(19)	Si(3)−N(51)−Si(4)	122.73(16)
Si(1)−O(1)−Li(2)	112.4(2)	O(1)−Li(1)−O(2)	100.4(3)
Si(1)−O(1)−Li(3)	162.9(2)	O(1)−Li(1)−N(21	92.1(2)
Li(1)−O(1)−Li(2)	85.1(3)	O(2)−Li(1)−N(21)	106.8(3)
Si(2)−N(21)−Li(1)	86.89(18)	Li(1)−O(1)−Li(3)	80.1(2)
Si(2)−N(21)−Li(2)	117.6(2)		

Table 5. Selected Interatomic Distances (Å) and Bond Angles (deg) for **3c·THF**

Si(1)−O(1)	1.621(3)	O(1)−Li(1)	1.886(7)
Si(1)−N(31)	1.770(4)	O(1)−Li(1)[a]	1.911(7)
N(21)−C(20)	1.427(5)	O(1)−Li(2)	1.859(5)
N(21)−Li(1)	2.004(8)	O(1)*−Li(1)	1.911(7)
N(21)−Li(2)[a]	2.046(8)	O(41)−Li(2)	1.872(14)
N(21)−Si(2A)	1.760(5)	N(31)−Si(2A)	1.786(4)
O(1)−Si(1)−N(31)	111.49(15)	Si(2A)−N(21)−Li(2)[a]	128.1(3)
N(21)−Si(2A)−N(31)	105.3(3)	C(20)−N(21)−Si(2A)	123.0(3)
Si(1)−O(1)−Li(1)	110.9(3)	O(1)−Li(1)−O(1)[a]	101.2(3)
Si(1)−O(1)−Li(2)	121.1(3)	O(1)−Li(1)−N(21)	126.9(4)
Si(1)−O(1)−Li(1)[a]	136.5(3)	O(1)[a]−Li(1)−N(21)	104.8(4)
Li(1)−O(1)−Li(1)[a]	78.8(3)	Li(1)−O(1)−Li(2)	123.7(3)
Si(1)−N(31)−Si(2A)	132.7(3)	Si(2A)−N(21)−Li(1)	112.7(3)

[a] Symmetry transformations used to generate equivalent atoms: $-x + 1, -y + 1, -z + 1$.

Table 6. Selected Interatomic Distances (Å) and Bond Angles (deg) for **4c**

N(21)−C(20)	1.419(3)	N(51)−Li(3)	2.041(5)
N(21)−Li(1)	1.992(5)	N(51)−Li(4)	1.998(6)
N(21)−Li(2)	2.010(5)	O(1)−Li(1)	1.782(5)
N(31)−Li(1)	2.219(5)	O(1)−Li(2)	1.991(5)
N(31)−Si(1)	1.778(2)	O(1)−Li(3)	1.851(5)
N(31)−Si(2)	1.782(2)	O(1)−Si(1)	1.620(2)
N(41)−Li(4)	2.240(5)	O(2)−Li(2)	1.842(5)
N(41)−Si(3)	1.789(2)	O(2)−Li(3)	1.985(5)
O(1)−Si(1)−N(31)	104.85(10)	O(2)−Li(4)	1.883(5)
N(21)−Si(2)−N(31)	101.35(11)	Si(2)−N(21)−Li(2)	124.18(19)
Si(1)−O(1)−Li(1)	93.86(18)	C(20)−N(21)−Li(1)	132.2(2)
Si(1)−O(1)−Li(2)	111.41(17)	O(1)−Li(1)−N(21)	100.0(2)
Si(1)−O(1)−Li(3)	140.25(19)	O(1)−Li(1)−N(31)	81.9(2)
Li(1)−O(1)−Li(2)	77.4(2)	O(1)−Li(2)−O(2)	96.1(2)
Si(2)−N(21)−Li(1)	90.59(18)	O(1)−Li(2)−N(21)	95.5(2)

Table 7. Selected Interatomic Distances (Å) and Bond Angles (deg) for **4c·3Et₂O**

Si(21)−N(11)	1.677(5)	N(11)−Li(1)	1.915(13)
Si(21)−N(31)	1.756(5)	O(11)−Li(1)	1.860(12)
Si(41)−N(31)	1.751(5)	O(11)−Li(2)	1.793(14)
Si(41)−O(11)	1.604(5)	Li(1)−O(51A)	1.893(19)
N(11)−C(11)	1.395(7)	Li(2)−O(61A)	2.00(2)
N(11)−Si(21)−N(31)	107.2(2)	Si(21)−N(11)−Li(1)	117.6(4)
O(11)−Si(41)−N(31)	112.9(2)	Si(41)−N(31)−Si(21)	124.0(3)
O(71A)−Li(2)−O(61A)	102.6(10)	Si(41)−O(11)−Li(2)	127.4(6)
C(11)−N(11)−Si(21)	126.2(4)	Si(41)−O(11)−Li(1)	112.5(5)
C(11)−N(11)−Li(1)	115.9(6)	Li(2)−O(11)−Li(1)	118.7(7)

dispersion coefficients are contained in the SHELXTL-NT 6.14[53] program library.

The non-hydrogen atoms were refined anisotropically. Hydrogen atoms on carbon atoms were included at geometrically idealized positions (C−H bond distances 0.95/0.98/1.00) and were not refined. The isotropic thermal parameters of the hydrogen atoms were fixed at 1.2 times that of the preceding carbon atom.

The plots for the crystal structures were generated using ORTEP-3.[54] The thermal ellipsoids in the ORTEP drawings are shown at the 33% probability level.

Results and Discussion

In general, two synthetic routes have been used to prepare symmetrical diamido [^{R}NON]$^{2-}$ ligands: a two-step lithiated

correction details can be found in the crystal information file (Supporting Information).

The structures were solved using direct methods and refined by full-matrix least-squares method on F^2 with SHELXL97-2.[52] Neutral atom scattering factors for non-hydrogen atoms and anomalous

(52) Sheldrick, G. M., *SHELXL97−2, Program for the Solution of Crystal Structures*; University of Göttingen: Göttingen, Germany, 1997.
(53) *SHELXTL-NT 6.14, XPREP, Program Library for Structure Solution and Molecular Graphics*; Bruker AXS Inc.: Madison, WI, 2000−2003.
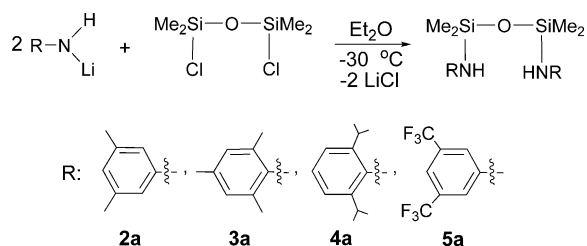(54) Farrugia, L. J. *J. Appl. Crystallogr.* **1997**, *30*, 565.

Table 8. Crystallographic Data

	compound						
	3a	**1c**	**1c·2THF**	**3c**	**3c·THF**	**4c**	**4c·3Et₂O**
formula	$C_{22}H_{36}N_2OSi_2$	$C_{40}H_{104}Li_8N_8O_4Si_8$	$C_{36}H_{84}Li_4N_4O_6Si_4$	$C_{44}H_{68}Li_4N_4O_2Si_4$	$C_{52}H_{84}Li_4N_4O_4Si_4$	$C_{56}H_{92}Li_4N_4O_2Si_4$	$C_{40}H_{76}Li_2N_2O_4Si_2$
fw	400.71	1041.52	809.18	825.14	969.35	993.46	719.09
cryst syst	monoclinic	triclinic	monoclinic	orthorhombic	triclinic	monoclinic	orthorhombic
space group	$P2_1/c$	$P\bar{1}$	$P\bar{1}$	$Pna2_1$	$P\bar{1}$	$P2_1/c$	$Pna2_1$
a, Å	18.4320(3)	12.05340(10)	10.5240(4)	30.5950(2)	12.8660(4)	20.3540(5)	19.4130(2)
b, Å	15.8940(7)	15.7902(2)	11.1990(3)	11.7650(2)	13.9530(3)	14.9220(4)	12.3350(4)
c, Å	8.3240(8)	17.6785(2)	11.9060(3)	13.3820(5)	16.9200(5)	24.6850(6)	19.0520(5)
α, deg	90	75.9850(10)	65.1620(17)	90	70.5380(18)	90	90
β, deg	93.129(3)	80.2350(10)	76.36608(17)	90	88.7260(12)	125.145(15)	90
γ, deg	90	85.4090(10)	77.9070(18)	90	89.5600(13)	90	90
V, Å³	2434.9(3)	3214.54(6)	1227.79(6)	4816.9(2)	2863.21(14)	6130.6(3)	4562.2(2)
Z	4	2	1	4	2	4	4
ρ_{calcd}, g/cm³	1.093	1.076	1.094	1.138	1.124	1.076	1.047
T, K	173	123	173	173	173	173	173
μ, cm⁻¹	0.159	0.206	0.162	0.161	0.147	0.137	0.114
$R(F)^a$ ($F_o^2 > 2\sigma(F_o^2)$)	0.0496	0.0367	0.0465	0.0477	0.0630	0.0534	0.0745
$R_w(F)^a$ ($F_o^2 > 2\sigma(F_o^2)$)	0.1108	0.0864	0.1126	0.0960	0.1565	0.1167	0.2067
GOF	1.026	1.020	1.035	1.039	1.023	1.021	1.051

a Function minimized $\sum w(|F_o|^2 - |F_c|^2)^2$ where $w^{-1} = [\sigma(F_o^2) + (nP)^2 + mP]$, $R = \sum||F_o| - |F_c||/\sum|F_o|$, $R_w = [\sum w(|F_o| - |F_c|)^2/\sum w|F_o|^2]^{1/2}$, $P = 1/3(F_o^2 + 2F_c^2)$, $n = 0.0436$ $m = 1.3415$ for **3a**, $n = 0.0484$ $m = 0.8117$ for **1c**, $n = 0.0506$ $m = 0.8236$ for **1c·2THF**, $n = 0.0325$ $m = 4.1228$ for **3c**, $n = 0.0799$ $m = 2.1186$ for **3c·THF**, $n = 0.0496$ $m = 3.1191$ for **4c**, $n = 0.1461$ $m = 2.5871$ for **4c·3Et₂O**.

Scheme 2

R: **2a**, **3a**, **4a**, **5a**

Figure 1. Molecular structure of **3a** (33% probability ellipsoids are shown; non-amino hydrogen atoms are removed for clarity).

Scheme 3

amide route and a one-pot excess amine route.[31,35,36,55] In order to systematically explore the electronic and steric impact of the amido R groups on the retro-Brook reactivity of these ligands that we recently reported,[24] we prepared new NON ligands with nonsteric propyl and moderately steric 3,5-Me₂Ph groups. In the case of the less basic arylamido R group, 3,5-Me₂Ph, the two-step lithium amide route was used to synthesize the respective diaminosilyl ether ligand precursor (Scheme 2), as was done for other arylamido-substituted systems. Thus, addition of 1,3-dichloro-1,1,3,3-tetramethyl-disiloxane at −30 °C to an ether solution of 3,5-Me₂PhNHLi resulted in the isolation of the dark orange oil H₂[^{Me_2Ph}NON] (**2a**).

Attempts to prepare the analogous R = propyl {[PrNH-(SiMe₂)]₂O} ligand via a similar procedure failed and instead resulted in a mixture of products. Thus, the excess amine route was employed, in which direct addition of 1,3-dichloro-1,1,3,3-tetramethyldisiloxane to an excess of neat anhydrous propylamine afforded a colorless oil H₂[^{Pr}NON] (**1a**) in high yield (Scheme 3). The addition of (ClSiMe₂)₂O to this highest concentration of propylamine results in rapid replacement of both Cl⁻ groups with external PrNH⁻. The propylamine
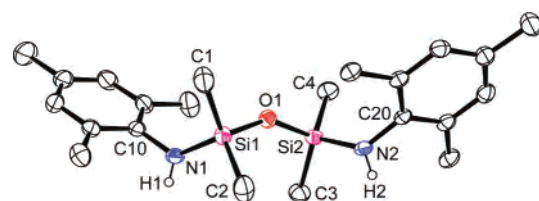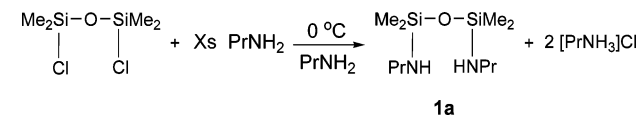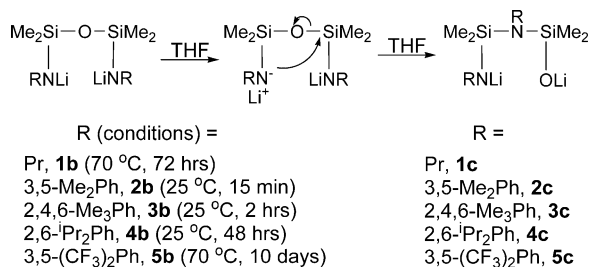
solvent also serves to mop up the HCl produced, generating a white precipitate of [PrNH₃]Cl. Note that the use of neat propylamine is key to the reaction's success; mixtures of products are obtained from silylchloride addition to ether/PrNH₂ solutions. The previously prepared R = ^{t}Bu and Ph analogues[35,36] use a similar amine-addition route, but excess amine is not required in those cases.

Compounds **1a** and **2a** were characterized by ¹H NMR, mass spectroscopy, and elemental analysis. The related diamidosilyl ether ligand precursors (Scheme 2) {[RNH-(SiMe₂)]₂O} (R = 2,4,6-Me₃Ph, H₂[^{Me_3Ph}NON] (**3a**); 2,6-^{i}-Pr₂Ph, H₂[^{iPr_2Ph}NON] (**4a**); 3,5-(CF₃)₂Ph, H₂[^{CF_3Ph}NON] (**5a**)) have been previously reported by our group,[31,55] but no solid-state structures were described. As a representative example, the solid-state structure of diaminosilyl ether **3a** was obtained; crystals were grown by cooling a saturated hexanes solution to −30 °C. An ORTEP structure of **3a** is shown in Figure 1; selected interatomic distances and bond angles are detailed in Table 1.

(55) Mund, G.; Gabert, A. J.; Batchelor, R. J.; Britten, J. F.; Leznoff, D. B. *Chem. Commun.* **2002**, 2990.
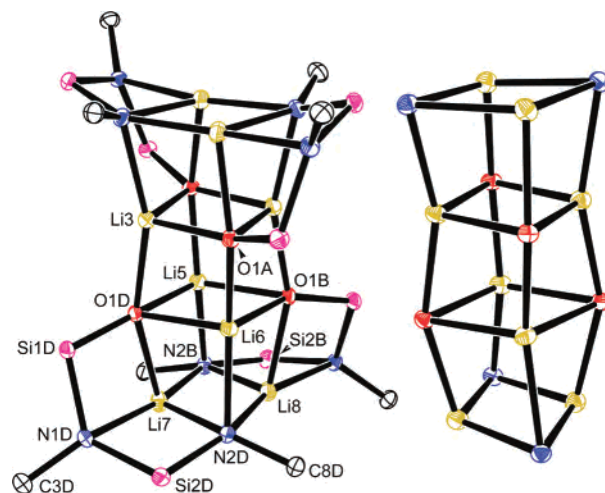
Scheme 4

R (conditions) =

Pr, **1b** (70 °C, 72 hrs)
3,5-Me$_2$Ph, **2b** (25 °C, 15 min)
2,4,6-Me$_3$Ph, **3b** (25 °C, 2 hrs)
2,6-^{i}Pr$_2$Ph, **4b** (25 °C, 48 hrs)
3,5-(CF$_3$)$_2$Ph, **5b** (70 °C, 10 days)

R =

Pr, **1c**
3,5-Me$_2$Ph, **2c**
2,4,6-Me$_3$Ph, **3c**
2,6-^{i}Pr$_2$Ph, **4c**
3,5-(CF$_3$)$_2$Ph, **5c**

The silyl ether backbone forms a twisted zigzag chain with trigonal planar nitrogen centers and an Si−O−Si bond angle similar to that of Me$_3$SiOSiMe$_3$.[56]

Deprotonation of **1a**−**5a** with 2 equiv of ^{n}BuLi in Et$_2$O or toluene yielded the *N*-lithio derivatives {[RNLi(SiMe$_2$)]$_2$O} (R = Pr, Li$_2$[^{Pr}NON] (**1b**); 3,5-Me$_2$Ph, Li$_2$[^{Me_2Ph}NON] (**2b**); 2,4,6-Me$_3$Ph, Li$_2$[^{Me_3Ph}NON] (**3b**); 2,6-^{i}Pr$_2$Ph, Li$_2$[^{iPr_2Ph}NON] (**4b**); 3,5-(CF$_3$)$_2$Ph, Li$_2$[^{CF_3Ph}NON] (**5b**)). However, if the lithiation reaction of compounds **1a**−**5a** is conducted in THF or if the isolated *N*-lithio derivatives of the ligands **1b**−**5b** are stirred in THF, they undergo an anionic intramolecular [1,3]-O → N silyl retro-Brook rearrangement[26] in which one silyl group migrates from oxygen to the amido nitrogen (Scheme 4). Thus, this reaction yields compounds of the form {RNLiSiMe$_2$N(R)SiMe$_2$OLi} (R= Pr, Li$_2$[^{Pr}NN′O] (**1c**); 3,5-Me$_2$Ph, Li$_2$[^{Me_2Ph}NN′O] (**2c**); 2,4,6-Me$_3$Ph, Li$_2$[^{Me_3Ph}NN′O] (**3c**); 2,6-^{i}Pr$_2$Ph, Li$_2$[^{iPr_2Ph}NN′O] (**4c**); 3,5-(CF$_3$)$_2$Ph, Li$_2$[^{CF_3Ph}-NN′O] (**5c**)); these can be viewed as new mixed-donor amido−amino−siloxo ligands prepared in one step and high yield.

The rearrangement reaction was confirmed by ^{1}H NMR spectroscopy. In the unrearranged form, the structure has mirror symmetry, and thus, a single resonance is observed for each set of symmetrical protons. However, in the rearranged form, the symmetry is lost, and therefore, two different peaks of equal intensity are observed for each set of protons.

As representative examples of nonsteric, relatively and extremely bulky amido−amino−siloxo ligands, single crystals of compounds **1c**, **3c**, and **4c** suitable for X-ray diffraction were obtained from the slow evaporation of saturated solutions of both donor (THF or Et$_2$O) and nondonor (pentane, hexanes, or toluene) solvents at room temperature in order to examine the effect of donor solvent on the structure and aggregation level of the salts. Thus, when recrystallized from toluene/pentane solution, in the solid state, **1c** forms a tetrameric cluster with a rare triple-stack of fused twisted cubes of lithium amide/siloxide (Figure 2).[57] The structure can also be regarded as an alternating stack of four Li$_2$N$_2$ and Li$_2$O$_2$ rings. The four central Li atoms are coordinated by one amide nitrogen and three siloxide oxygen atoms. The four outer lithium atoms are coordinated by one siloxide oxygen, two amide nitrogens and one amine nitrogen atom. Thus, the ligands bind to the terminal lithium centers

(56) Barrow, M. J.; Ebsworth, E. A. V.; Harding, M. M. *Acta Crystallogr.* **1979**, *B35*, 2093.
(57) Marsch, M.; Harms, K.; Lochmann, L.; Boche, G. *Angew. Chem., Int. Ed. Engl.* **1990**, *29*, 308.

Figure 2. (left) Molecular structure of the tetrameric cluster of **1c** (33% probability ellipsoids are shown; alkyl groups are simplified for clarity). (right) Simplified triple-stacked lithium cubane of the structure's core.
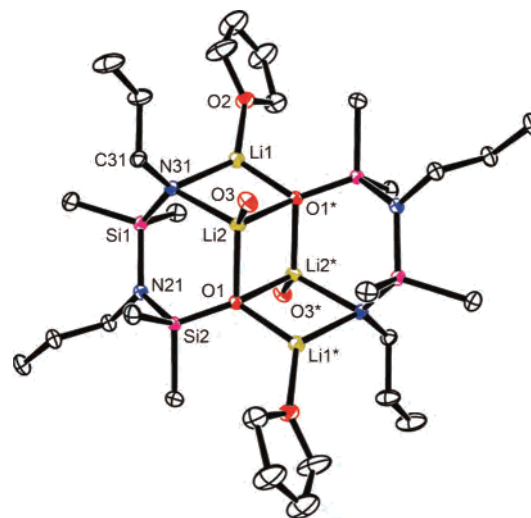
Figure 3. Molecular structure of **1c·2THF** (ORTEP view with 33% probability ellipsoids are shown; O3-THF groups simplified for clarity).

in a tridentate fashion. The Li(7)−N(1D)$_{amine}$ bond of 2.224-(3) Å is significantly longer than the amido Li(7)−N(2B) and Li(7)−N(2D) bonds of 2.050(3) and 2.084(3) Å (Table 2).[58−60]

However, recrystallization of **1c** from THF/toluene solution resulted in single crystals of the THF adduct {Li$_2$[^{Pr}-NN′O]·THF$_2$}$_2$ (**1c·2THF**). The lithium ion solvation by the THF donors inhibits the ring-stacking observed for the previous base-free structure and yields a dimeric system with a ring-laddering motif (Figure 3), consisting of a lateral attachment of two Li−N−Li−O rings or, alternatively, four Li−N and Li−O rungs.[61−63] The central ring of the ladder,

(58) Pauer, F.; Power, P. P. In *Lithium Chemistry: A Theoretical and Experimental Overview*; Sapse, A.-M., Schleyer, P. v. R., Eds.; Wiley-Interscience: New York, 1995; p 295.
(59) Becker, G.; Hitchcock, P. B.; Lappert, M. F.; MacKinnon, I. A. *J. Chem. Soc., Chem. Commun.* **1989**, 1312.
(60) Grotjahn, D. B.; Sheridan, P. M.; Al, Jihad, I.; Ziurys, L. M. *J. Am. Chem. Soc.* **2001**, *123*, 5489.
(61) Hursthouse, M. B.; Hossain, M. A.; Motevalli, M.; Sanganee, M. *J. Organomet. Chem.* **1990**, *381*, 293.
(62) Armstrong, D. R.; Barr, D.; Clegg, W.; Mulvey, R. E.; Reed, D.; Snaith, R.; Wade, K. *J. Chem. Soc., Chem. Commun.* **1986**, 869.
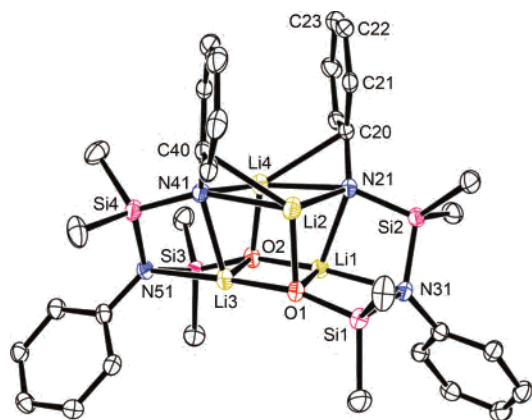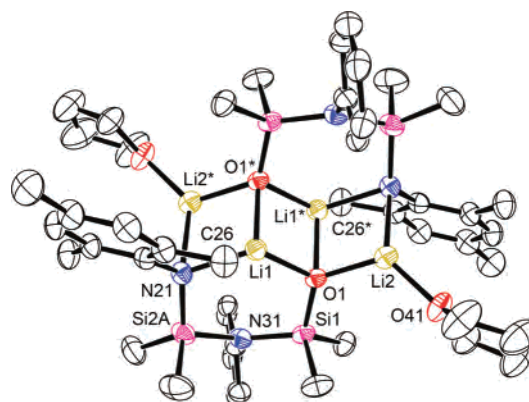
Figure 4. Molecular structure of **3c** (ORTEP view with 33% probability ellipsoids are shown; aryl groups simplified for clarity).
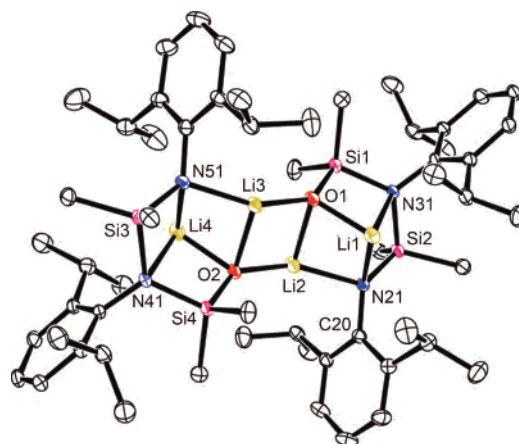

Figure 5. Molecular structure of **3c·THF** (ORTEP view with 33% probability ellipsoids are shown; N31-aryl groups simplified for clarity).

Figure 6. Molecular structure of **4c** (ORTEP view with 33% probability ellipsoids are shown).

Li(2)−O(1)−Li(2)*−O(1)*, is planar, with the outer rings straddling this plane on opposite sides in a stair-shaped fashion. The O−Si−N−Si−N backbone acts as a bidentate chelate; in other words, the central silylamine does not bind to any lithium, unlike in solvent-free **1c**.

When **3c** was recrystallized from nondonor toluene/hexanes solution, another solvent-free stacked structure was observed (Figure 4). Due to the higher degree of steric constraint imposed by mesityl compared to propyl groups, the structure is a dimer and consists of a $Li_4N_2O_2$ heterocubane fused by two tridentate, chelating ligands at opposite sides of the core cubane. The average $Li-N_{amine}$ bond length of 2.270 Å in **3c** is slightly longer than in solvent-free **1c** (2.165 Å), reflecting both the increased steric hindrance and reduced basicity of **3c** vs **1c**.[64] Interestingly, the Li(2) and Li(4) centers participate in Li(2)−C(40) and Li(4)−C(20) ipso interactions, as indicated by an average bond length of 2.421 Å and an average, very acute $Li-N_{amido}-C_{ipso}$ angle of 79.25°. As a result, the aromaticity in the activated mesityl rings is also partially disrupted (see Table 4 for C−C values).[65]

Recrystallization of **3c** from THF/toluene solution gave single crystals of the THF adduct {Li_2[^{Me_3Ph}NN′O]·THF}$_2$ (**3c·THF**). As with **1c**, the complexation of THF molecules inhibits stacking, although the nuclearity does not decrease in this case: the structure of **3c·THF** is similar to that of **1c·2THF** and consists of a central dimeric ladder fused by two six-membered rings on opposite sides (Figure 5). However, the higher steric bulk of the mesityl groups prevent complexation of inner Li(1) and Li(1)* centers by THF donors. As in **1c·2THF**, the ligand backbone acts as a bidentate chelate, i.e., the central silylamine remains unbound to the inner Li centers. Instead, these lithium centers are additionally stabilized by an agostic methyl C(26)−

H(26)⋯Li(1) interaction, as indicated by the relatively short Li−C distance of ∼2.50 Å.[66−68]

The unsolvated dimeric structure of **4c** is shown in Figure 6. Unlike **1c** and **3c**, the Li_2O_2 and Li_2N_2 rings cannot stack into a cubane structure due to the higher steric bulk of the diisopropylphenyl groups compared to mesityl and a very distorted ladder-type dimer similar to the donor adducts **1c·2THF** and **3c·THF** is favored. The terminal lithium centers also form N_{amine}−Li bonds with an average length of 2.229 Å; hence, the ligand also acts as a tridentate chelate for the terminal lithium centers in this case.

Crystallization of **4c** from diethylether generated a solvated monomer {Li_2[^{iPr_2Ph}NN′O]·(Et$_2$O)$_3$} (**4c·3Et$_2$O**), as shown in Figure 7. The highly sterically encumbering 2,6-^{i}Pr$_2$ groups on the aromatic ring and higher degree of solvation per ligand compared to that of **1c·2THF** and **3c·THF** prevent any aggregation of the molecules in the solid state. The ligand acts as a bidentate chelate to Li(1), with an unbound central amine and a bridging siloxide to Li(2). The structure is further stabilized by complexation of three Et$_2$O molecules: one to Li(1) and two to Li(2).

(63) Armstrong, D. R.; Barr, D.; Clegg, W.; Hodgson, S. M.; Mulvey, R. E.; Reed, D.; Snaith, R.; Wright, D. S. *J. Am. Chem. Soc.* **1989**, *111*, 4719.

(64) Perrin, D. D. *Dissociation Constants of Organic Bases in Aqueous Solution*; Butterworths: London, 1965.

(65) Antolini, F.; Hitchcock, P. B.; Lappert, M. F.; Merle, P. *Chem. Commun.* **2000**, 1301.

(66) Armstrong, D. R.; Clegg, W.; Mulvey, R. E.; Barr, D.; Snaith, R. *J. Chem. Soc., Chem. Commun.* **1984**, 285.

(67) Armstrong, D. R.; Mulvey, R. E.; Walker, G. T.; Barr, D.; Snaith, R. *J. Chem. Soc. Dalton Trans.* **1988**, 617.

(68) Chen, H.; Barlett, R. A.; Deas, H. V. R.; Olmstead, M. M.; Power, P. P. *Inorg. Chem.* **1991**, *30*, 2487.
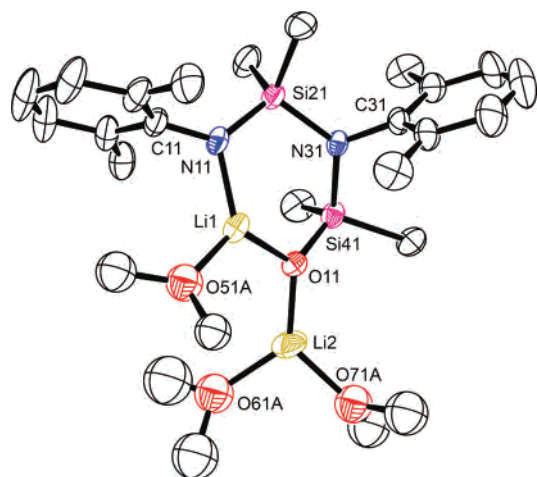
Figure 7. Molecular structure of **4c·3Et₂O** (ORTEP view with 33% probability ellipsoids are shown; diisopropyl groups and ether molecules are simplified for clarity).

It can be concluded from this body of structural information that the degree of aggregation in these lithium amido−amino−siloxo ligands is largely dictated by the steric constraints imposed by the R groups and the degree of solvation, as has been previously observed for simpler lithium amides.[5,44,69] In general, higher aggregation is observed when less bulky substituents (e.g., propyl) at the nitrogen centers are employed. The degree of aggregation also increases when the ligands are crystallized out of nondonor solvents such as toluene or hexanes. The structural studies also revealed that the chelating amido−amino−siloxo ligands are able to bind to lithium centers in both bidentate and tridentate modes. In particular, all three solvent-free systems contained tridentate (amido−amino−siloxo) ligands while incorporation of THF or ether donor solvents invariably triggered the release of the central silylamine unit from the lithium center, yielding only bidentate ligands. This preference for THF and even ether donors is likely a reflection of a combination of the oxophilicity of lithium cations and the relatively poor donor ability (due in part to steric restrictions or ring strain associated with binding etc.) of the silylamine.

NMR Studies. In order to study the degree of aggregation and complexation in solution, variable-temperature ^{7}Li and ^{1}H NMR spectra were recorded for **1c**, **3c**, and **4c** in THF-d_8 and toluene-d_8 at high concentrations. ^{13}C{^{1}H} NMR spectra were also recorded for the **1a**−**c** series. The ^{1}H NMR spectra of the same ligand salt in the two different solvents exhibit different chemical shifts, and the more structurally sensitive ^{13}C{^{1}H} NMR spectra showed a different number of peaks for **1c** in toluene vs THF, all consistent with different solvate structures existing in each solvent. As further evidence of this, the chemical shifts of the ^{7}Li NMR spectra in toluene-d_8 are all significantly shifted downfield (δ −0.41 to +1.53 at 298 K) compared to those in THF-d_8 (δ −0.81 to −1.83 at 298 K), and although it is difficult to correlate each chemical shifts to a specific Li site (i.e., THF-, siloxo-, or amido-bound Li centers)[70−72] due to the small chemical
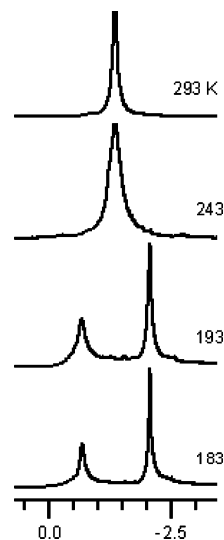
Figure 8. Variable-temperature ^{7}Li NMR spectra of **3c** in THF-d_8.

shift range for ^{7}Li, a similar toluene vs THF chemical shift trend was observed for a series of lithium sulfenamides.[72]

The variable-temperature NMR data were not especially informative about the nature of the structure in solution. For all compounds, peaks in the ^{1}H NMR spectra show only slight shifting and broadening (i.e., no new peaks or coupling) as a function of temperature. However, the ^{7}Li NMR spectra in toluene-d_8 indicated that some fast intramolecular fluxionality and/or intermolecular aggregation equilibria (for **1c** and **3c**) or a static system (**4c**) is present, but the nature of the fluxionality or aggregation level could not be determined.[5,73,74] In THF-d_8, the ^{7}Li NMR spectra all show fluxional behavior: **3c** shows two peaks at 183 K (δ −0.68, −2.06) and **4c** shows two peaks at 298 K (δ −1.83, −0.81), likely due to Li−amide and Li−siloxide groups.[46,75,76] Upon raising the temperature, coalescence to a single peak (δ −1.35 at 243 K for **3c** and −0.86 at 323 K for **4c**) is observed (representative spectra for **3c** are shown in Figure 8). For **1c**, the situation is more complex than for the bulkier **3c** or **4c** (see Experimental Section for ^{7}Li NMR data), and since both intramolecular fluxionality and some cluster dissociation/association equilibria are plausibly occurring simultaneously in **1c** in THF-d_8 we have not made any further attempts to interpret its ^{7}Li NMR spectra. However, examining the coalescence temperatures for the putative intramolecular fluxionality process, namely 173, 243, and 323 K for **1c**, **3c**, and **4c** respectively, indicates that the kinetic barrier increases with the steric hindrance of the amido R group. Unfortunately, further details of this process and the nuclearity of the lithiated ligands could not be unambiguously

(69) Cole, M. L.; Davies, A. J.; Jones, C.; Junk, P. C. *J. Organomet. Chem.* **2004**, *689*, 3093.
(70) Cox, R. H.; Terry, H. W. *J. Magn. Reson.* **1974**, *14*, 317.
(71) Lindman, B.; Forsen, S. In *NMR and the Periodic Table*; Harris, R. K., Mann, B. E., Eds.; Academic Press: London; New York, 1978; p 166.
(72) Mahmoudkhani, A. H.; Rauscher, S.; Grajales, B.; Vargas-Baca, I. *Inorg. Chem.* **2003**, *42*, 3849.
(73) Roussel, P.; Alcock, N. W.; Scott, P. *Inorg. Chem.* **1998**, *37*, 3435.
(74) Fryzuk, M. D.; Hoffman, V.; Kickham, J. E.; Rettig, S. J.; Gambarotta, S. *Inorg. Chem.* **1997**, *36*, 3480.
(75) Boman, A.; D., J. *Magn. Reson. Chem.* **2000**, *38*, 853.
(76) Zabicky, J. In *The Chemistry of Organolithium Compounds*; Rappoport, Z., Marek, I., Eds.; Wiley: New York, 2004.

Table 9. Summary of the Kinetic Parameters for Rearrangement Reactions of Compounds **1b−5b** to **1c−5c**

R group	$\Delta H^{\ddagger}$ kJ/mol	$\Delta S^{\ddagger}$ J/K·mol	$\Delta G^{\ddagger}$ kJ/mol	E_a kJ/mol	$\tau_{1/2}{}^a$ s
Pr (**1**)	79	−80	103	82	3.8×10^6
Me₂Ph (**2**)	51	−111	84	53	5.7×10^1
Me₃Ph (**3**)	67	−72	88	69	3.1×10^2
^{i}Pr₂Ph (**4**)	78	−62	97	79	9.3×10^3
(CF₃)₂Ph (**5**)	117	−12	121	120	1.5×10^8

^{a} At 298 K.

determined in either toluene or THF from the multinuclear, variable-temperature NMR data.

Kinetic Study of the Retro-Brook Rearrangement of Li₂[^{R}NON] to Li₂[^{R}NN′O]. The kinetic parameters of the retro-Brook rearrangement reactions for *N*-lithio derivatives of the ligands **1c−5c** were determined by peak integration analysis of the ^{1}H NMR spectra in THF-d_8 taken during the course of the reactions at three different temperatures. Plots of ln(Li₂[^{R}NON]) vs time were nearly linear, indicating that the rearrangement reaction follows a first-order process. Changing the concentration of the NMR sample had no effect on the rate of the rearrangement; comparable kinetic data was obtained using 10, 20, and 30 mg/mL (Li₂[^{R}NON]/THF-d_8) concentrations. Furthermore, no other products were detected in the ^{1}H NMR spectra. Both of these points indicate that the rearrangement is predominantly an intramolecular process. The well-known retro-Brook reaction mechanism starts with lithium abstraction from an amide group by THF. The generated nucleophile then attacks silicon intramolecularly, creating a five-coordinate transition state at silicon, which eventually leads to a new rearranged ligand after the Si−O bond is broken. The values of $\Delta H^{\ddagger}$, $\Delta S^{\ddagger}$, $\Delta G^{\ddagger}$, E_a, and $\tau_{1/2}$ for the rearrangement reaction of the Li₂[^{R}NON] ligands are summarized in Table 9.[25]

The half-life, $\tau_{1/2}$, values at room-temperature fall in the broad range of seconds to days, expressing the significance of steric and electronic effects of the amido R substituent on the rearrangement reaction. Activation energies are relatively low (53−120 kJ/mol) which suggests that the transition state is of relatively low energy.[25] The greater ionic stability of the lithium siloxide compared to the starting lithium amide presumably offsets the energy required to break a Si−O and form a weaker Si−N bond (444 and 318 kJ, respectively).[77] Furthermore, the $\Delta S^{\ddagger}$ values are relatively large and negative, −12 to −111 J/K·mol depending on the system, suggesting considerable reduction of freedom in the transition state.[25]

In order to qualitatively determine the relative importance of steric vs electronic effects on the rate, subsets of the data can be compared. For example, the $\tau_{1/2}$ values for the highly electron-withdrawing, weakly nucleophilic **5b** vs the electron-rich **2b**, both of which have similarly low steric profiles, are 1.5×10^8 and 5.7×10^1 s, respectively; i.e. the electron-rich **2b** reacts nearly 2.5×10^6 times faster than the electron-poor **5b**. Indeed, these two examples span the widest range of kinetics and $\Delta G^{\ddagger}$ barriers.

Compounds **2b**, **3b**, and **4b** have relatively similar electronic properties, but increasing steric hindrance at the amide centers. Accordingly, the values of $\tau_{1/2}$ and $\Delta G^{\ddagger}$ increase from **2b** to **3b** to **4b** as the steric hindrance increases. However, despite the large steric impediment generated by 2,6-^{i}Pr₂ groups compared to the 3,5-Me₂Ph substituents, the $\tau_{1/2}$ values only increase by a factor of ~160 and are still ~10^4 faster than the less bulky 3,5-(CF₃)₂Ph-containing **5b**. In summary, electronic effects at the nucleophilic amido nitrogen appear to be more important than steric hindrance in influencing the kinetics of the retro-Brook rearrangement in this case.

The propyl substituent in **1b** yields the most nucleophilic amide among the ligands studied, and it also exerts the least steric hindrance of any R group presented here. Thus, it could be expected that **1b** should have the fastest rearrangement, yet the rearrangement of Li₂[^{Pr}NON] occurs with a greater $\Delta G^{\ddagger}$ and $\tau_{1/2}$ (103 kJ/mol and 3.8×10^6 s, respectively) than all others except the fluorinated ligand **5b**. In the solid state, Li₂[^{Pr}NN′O] has the highest tendency to aggregate, and this aggregation presumably exists to some degree in solution for the non-rearranged form as well.[46−49] Thus, the energy barrier required to break up any aggregated clusters of Li−N bonds prior to intramolecular attack on silicon may inhibit the rearrangement process. It is also possible that the relatively high nucleophilicity of the amido nitrogen in **1b** may increase the Li−N ionic bond strength and prevent dissociation of Li$^+$ from the amide in THF, also inhibiting rearrangement.

Finally, the rearrangement of Li₂[^{tBu}NON][50,51] was attempted in THF-d_8, but no reaction was observed. Despite the high nucleophilicity of the N-donor, presumably the steric bulk of the ^{t}Bu completely inhibits the intramolecular nucleophilic attack on Si, or equally likely, the putative final product, containing a Me₂Si−N(^{t}Bu)−SiMe₂ backbone is simply too sterically strained to form at all.

These observations are consistent with prior studies on the mechanism of the Brook-type rearrangement reactions;[25,26,77−81] in general, increasing the nucleophilicity of the amido nitrogen decreases the activation energy for intramolecular attack on silicon and thus increases the rate of the rearrangement. Other reported activation energies for anionic Brook-type rearrangements are fairly low, but entropies of activation are large and negative, as in this system.[25] For instance, the rates of rearrangement of [R₃SiCR′₂O]$^-$ (R and R′ = H, Me, Phenyl) showed that the energies of activation, E_a, were of the order of 33−46 kJ/mol and the $\Delta S^{\ddagger}$ were of the order of −146 to −167 J/K·mol depending on the R groups.[27]

Conclusion

New symmetrical alkyl- and aryl-substituted diamidosilyl ether ligands were synthesized by two distinct routes: an excess amine route and a lithiated amide pathway. The retro-

(77) West, R.; Boudjouk, P. *J. Am. Chem. Soc.* **1973**, *95*, 3987.

(78) Brook, A. G.; LeGrow, G. E.; MacRae, D. M. *Can. J. Chem.* **1967**, *45*, 239.
(79) Duff, J. M.; Brook, A. G. *Can. J. Chem.* **1973**, *51*, 2869.
(80) West, R.; Bichlmeir, B. *J. Am. Chem. Soc.* **1972**, *94*, 1649.
(81) Wright, A.; West, R. *J. Am. Chem. Soc.* **1974**, *96*, 3214.

Brook rearrangement reaction was employed to synthesize a new class of nonsymmetrical mixed-donor amido−amino−siloxo ligands {RNLiSiMe$_2$N(R)SiMe$_2$OLi} in one facile step and in high yield, which can act as both bidentate amido−siloxo or tridentate chelates. A structural study of the dilithiated mixed-donor amido−amino−siloxo ligands **1c**, **3c**, and **4c** with and without donor solvent indicated that these salts can adopt a range of structural motifs from a single-ring monomer to a tetrameric cluster. The extent of aggregation is dictated by the steric crowding about the lithium centers and the presence/absence of donor solvent. The kinetic parameters of the retro-Brook rearrangement reactions for *N*-lithio derivatives of the ligands indicated that the rate of rearrangement increases with decreasing steric hindrance and increasing electron-donating ability of the R substituent.

The use of the Brook rearrangement to generate new, unusual mixed-donor ligands in high yield indeed appears to be general and can be utilized in future mixed-donor ligand design and subsequent coordination chemistry.

Supporting Information Available: Crystallographic data in CIF format. This material is available free of charge via the Internet at http://pubs.acs.org.

IC701267A